

## PRELIMINARY MODELING OF AIR BREAKDOWN WITH THE ICEPIC CODE

A.E. SCHULZ<sup>1,2</sup>, A.D. GREENWOOD<sup>1</sup>, K.L. CARTWRIGHT<sup>1</sup>, P.J. MARDAHL<sup>1</sup>, R.E. PETERKIN<sup>1</sup>, N. BRUNER<sup>3</sup>, T. GENONI<sup>3</sup>, T.P. HUGHES<sup>3</sup>, D. WELCH<sup>3</sup><sup>1</sup>Air Force Research Laboratory, Directed Energy Directorate, Kirtland AFB, NM 87117<sup>2</sup>Department of Physics, Harvard University, Cambridge, MA 02138<sup>3</sup>Mission Research Corporation, Albuquerque, NM 87110

## ABSTRACT

Interest in air breakdown phenomena has recently been re-kindled with the advent of advanced virtual prototyping of radio frequency (RF) sources for use in high power microwave (HPM) weapons technology. Air breakdown phenomena are of interest because the formation of a plasma layer at the aperture of an RF source decreases the transmitted power to the target, and in some cases can cause significant reflection of RF radiation. Understanding the mechanisms behind the formation of such plasma layers will aid in the development of maximally effective sources. This paper begins with some of the basic theory behind air breakdown, and describes two independent approaches to modeling the formation of plasmas, the dielectric fluid model and the Particle in Cell (PIC) approach. Finally we present the results of preliminary studies in numerical modeling and simulation of breakdown.

## 1. INTRODUCTION

The subject of RF breakdown of air is one of particular interest to any current effort in designing a device to project a high power electromagnetic signal over some distance through the atmosphere. In the case of high power microwave devices, air breakdown interferes with the transmission of RF power, and in some cases reflects a large fraction of that power back toward the source. It is useful to study the details of how the breakdown occurs in order to answer several important questions. At what point after initial exposure to the RF signal does the breakdown occur? What field intensities cause it to begin? What densities are reached, and what is the density profile throughout the gas being ionized? What ionization states are produced? How do the properties of the medium change, and what is the net effect on the propagation of the RF signal?

To begin answering these questions, it is necessary to investigate the air chemistry and types of interactions that electrons driven by the RF fields

will have with the surrounding gas, and also with the device emitting the RF signal. High-energy electrons and ions that collide with background neutral gas molecules can cause impact ionization. High-energy electrons that collide with solid walls can produce secondary electrons. Both types of collision events have the potential to modify the plasma density, and hence can influence the physical behavior of the device under investigation. Thus, for more realistic numerical simulations, we have begun to develop numerical models for both of these time-dependent plasma formation processes. Including these effects will be crucial for any future virtual prototyping of high power microwave devices, currently in development at the Air Force Research Laboratory. Understanding how the properties of the medium change will allow us to maximize the effectiveness of microwave source design.

In this paper we begin a careful investigation of the physics behind breakdown processes. Section 2 outlines some basic theory surrounding the physics of breakdown. Section 3 describes our modeling techniques for propagating an electromagnetic signal through a medium, including a bulk treatment of the plasma as a dielectric fluid, and also a model of plasma electrons using a Particle in Cell (PIC) approach. Section 4 includes an investigation of the role of the collision frequency in the breakdown process. Also in section 4 we present the results of a full breakdown simulation in helium, a simpler gas than air, employing the dielectric fluid breakdown model. Finally in section 5 we draw conclusions and outline plans for future research.

## 2. BREAKDOWN BASICS

The basic mechanism of RF breakdown is a catastrophic growth in the density of electrons in the medium, driven by the energy taken from the incident electromagnetic signal. Several conditions are necessary for this process to occur efficiently; there

must be a significant population of background electrons to begin the ionization avalanche, there must be sufficient energy in the wave to impart ionizing energies to the electrons being accelerated, and the rate at which the background gas is being ionized must exceed the rates at which electrons are lost through attachment, diffusion and recombination. The evolution of the number density is governed by the equation

$$\frac{\partial N_e}{\partial t} = \lambda + \nu_i N_e - \nu_a N_e - \nu_d N_e - \zeta N_e^2 \quad (1)$$

where the terms are:  $\lambda$ , the quiescent generation of electrons due to background radiation such as cosmic rays,  $\nu_i$ , the ionization frequency,  $\nu_a$ , the attachment frequency,  $\nu_d$ , the diffusion frequency, and  $\zeta$ , the recombination rate constant. At atmospheric temperatures and pressures  $\nu_a \gg \nu_d$  and  $\nu_a \gg \zeta N_e$ , so attachment is the loss mechanism which imposes the strongest constraint on the breakdown threshold. The ionization and attachment frequencies are given by

$$\nu_i = \frac{\alpha e E_{eff}}{m \nu_c} \quad (2)$$

$$\nu_a = \frac{\beta e E_{eff}}{m \nu_c} \quad (3)$$

where

$$E_{eff}^2 = \frac{E_{rms}^2}{1 + \omega^2 / \nu_c^2} \quad (4)$$

Here  $\nu_c$  is the collision frequency that includes all momentum transferring events, and  $\alpha$ ,  $\beta$ , and  $\nu_c$  all depend on the mean electron energy  $W$ , which evolves according to the equation

$$\frac{dW}{dt} = \frac{e^2 E_{eff}^2}{m \nu_c} - \frac{2m}{M} \nu_c W - \nu_i W \quad (5)$$

The first term in this equation represents the energy gained under the influence of the RF field, and the loss terms are from inelastic collisions and ionizing collisions respectively. Functional forms for  $\alpha$  and  $\beta$  and much of the theory presented in this section can also be found in Anderson et. al. 1984.

Just how the concept breakdown is defined is a matter of some debate. The conventional wisdom is that when the electron density becomes so large that the plasma frequency grows comparable to the frequency of the RF radiation, the signal can no longer propagate through the medium, and breakdown has occurred. We agree that interference with the propagation of the signal is an adequate definition of breakdown. However we shall demonstrate later in this section that because the electrons suffer collisions with the background gas molecules, the

threshold at which the propagation is impacted can sometimes correspond to plasma frequencies that are considerably higher than the frequency of the RF signal. Nonetheless, for the purposes of developing some intuition about breakdown it is useful to compare the plasma frequency with the RF frequency.

The extent of the breakdown that occurs depends somewhat on whether the medium is exposed to a continuous or a pulsed RF signal. The breakdown criterion for a continuous signal is simply that  $\partial n / \partial t > 0$ . Because the signal never shuts off, there is no time limit and the plasma frequency will eventually grow to be comparable to the continuous wave frequency, and thus affect the signal. The only condition for breakdown via continuous RF radiation is that the energy be large enough to ionize more electrons than are being lost to attachment, diffusion, and recombination.

The breakdown criterion for a single pulse is a little more complex but not difficult to understand. Because of the limited pulse length,  $\tau$ ,  $dn/dt$  must be large enough to make  $\omega_p \sim \omega_{RF}$  on timescales less than  $\tau$ . If this condition is not met, the pulse will pass through the medium unaffected. The rate of density growth depends on the mean electron energy  $W$ , which depends on the field strength. Therefore, shorter pulses will require higher field strengths than longer ones in order to suffer breakdown effects. When breakdown occurs in a pulse, the effect is typically that the back portion is either absorbed or reflected, which is often referred to as tail erosion. Fig. (1) depicts the passage of a square pulse through a region of gas which in time is getting ionized and affecting the pulse shape. At early times, the gas has a small ionization fraction and is virtually transparent to the incident electromagnetic signal, which explains why the front portion of the pulse is unaffected. The radiation accelerates the few existing electrons, and begins to lose its energy to heating and ionization of the background gas molecules. As the electron density grows, the plasma begins to reflect an increasing fraction of the incident wave, resulting in smaller transmitted power. This is responsible for eroding the back half of the pulse.

The breakdown criterion for repeated pulses is similar to that of the single pulse, with the added complication that while the signal is off, the electron density is decreasing because of the attachment, diffusion, and recombination loss mechanisms. Multiple pulses relax the requirement on  $\partial N_e / \partial t$  since the driving field will return several times to feed energy into the plasma. The breakdown requirement therefore depends both on pulse length  $\tau$  and on the pulse repetition frequency  $\tau_{prf}$ . During the time when the

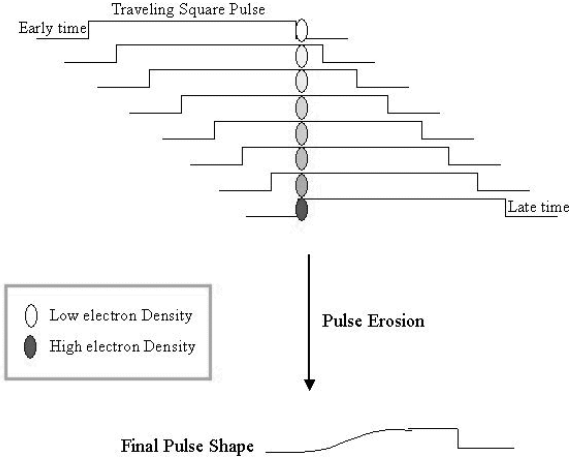


FIG. 1.— This cartoon shows how the passage of a pulse through a region of gas causes ionization of the gas and an increase in the electron density. As the electron density grows, more of the energy in the pulse is being absorbed or reflected, changing the shape of the wave-form that is transmitted through the region.

pulse is off  $\tau_{prf} - \tau$ , the electron density is decaying, so the breakdown criterion for an infinite string of pulses will be that  $\Delta N_e(\text{on}) > \Delta N_e(\text{off})$ .

Introducing collisions into the picture complicates things substantially. The effect of a high collision frequency  $\nu_c$  is to retard the rate of density growth, and also to retard the erosion of the transmitted signal. To understand this, consider first that a high collision frequency means that the mean free path and the mean free time between collisions are both very short. One effect of the short mean free time is that the electron being accelerated in the RF field does not often have time to gather sufficient energy to ionize a gas molecule before it collides again. Each time it collides, it loses whatever small energy it gained in the acceleration to the neutral atom it collided with, so ionizing events become much rarer. For the same reason, the electrons are also much less efficient at removing energy from the RF signal and dumping it into heating of the gas.

A consequence of the short mean free path resulting from a high collision frequency is that the electrons become much less mobile. Confining the electrons close to their original locations effectively makes the plasma behave less like a metal than when the electrons are highly mobile. The frequent collisions prevent the electrons from displacing from their ion friends and counteracting the incident field. Thus, a high collision frequency greatly decreases the efficiency of reflecting the signal, even when the electron densities are so high that  $\omega_p \sim \omega_{RF}$ . Fig. (2) illustrates this point by showing the net transmitted signal through a plasma layer as a function of the collision frequency

with the background gas. The plasma is held at a constant density, corresponding to a plasma frequency of  $\omega_p = 21.45$ . On the left side of the plot the transmission coefficients asymptote to their values in the collisionless regime. Four of the frequencies plotted are above the plasma frequency, whereas the fifth is below it, and in the collisionless case would be perfectly reflected by the plasma layer. In the case of the four transmitting frequencies, when the collision frequency is increased (corresponding perhaps to a higher density of background gas) the signal is being absorbed into heating of the background gas. Notice however that as the collision frequency is increased further, the mobility and energy transfer of the electrons is so hampered that all the frequencies begin to transmit through the plasma layer, regardless of whether  $\omega_p$  is less than or greater than  $\omega_{RF}$ .

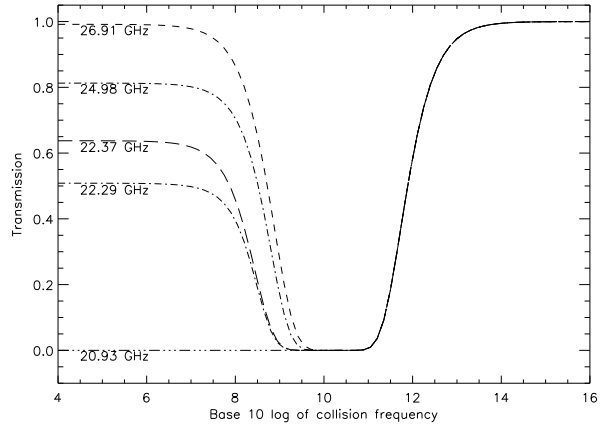


FIG. 2.— The theoretical prediction for the transmission coefficient for several different RF frequencies as a function of the collision frequency  $\nu_c$  of electrons in the plasma with background neutral gas. The plasma density is held fixed, with a plasma frequency of  $\omega_p = 21.45$  GHz.

### 3. METHOD

#### 3.1. The Dielectric Fluid Model

For dense plasmas, it is a good approximation to treat the plasma as a fluid with a frequency dependent dielectric constant. In the presence of EM radiation, this approximation is good for time-scales over which the fluid moves a small amount. The dielectric constant used in the fluid approximation is (in terms of the permittivity of free space  $\epsilon_0$ , the collision frequency  $\nu_c$ , and the frequency of the elec-

tromagnetic radiation  $\omega_{\text{EM}}$ )

$$\epsilon = \epsilon_0 \left( 1 - \frac{\omega_p^2}{\omega_{\text{EM}}(\omega_{\text{EM}} + i\nu_c)} \right) \quad (6)$$

where the plasma frequency  $\omega_p$  depends on the density  $n_0$  and species  $(m, q)$  of the ionized particles, and is given by  $\omega_p^2 = n_0 q^2 / m \epsilon_0$ .

To model high density plasma in the time domain, consider Ampere's law with the plasma dielectric constant;

$$\nabla \times \mathbf{B}(\mathbf{x}, \omega) = \mu_0 \epsilon_0 \left( -i\omega + \frac{\omega_p^2}{\nu_c - i\omega} \right) \mathbf{E}(\mathbf{x}, \omega) \quad (7)$$

The equivalent expression in the time domain is given by

$$\begin{aligned} \nabla \times \mathbf{B}(\mathbf{x}, t) = & \mu_0 \epsilon_0 \frac{\partial \mathbf{E}(\mathbf{x}, t)}{\partial t} \\ & + \omega_p^2 \mu_0 \epsilon_0 \int_{-\infty}^t e^{-\nu_c(t-\tau)} \mathbf{E}(\mathbf{x}, \tau) d\tau \end{aligned} \quad (8)$$

Differentiating Eq. (8) with respect to time and substituting the result back into Eq. (8) eliminates the convolution integral and yields the following expression used to define the field update equations in the dielectric fluid model.

$$\begin{aligned} \frac{\partial^2 \mathbf{E}(\mathbf{x}, t)}{\partial t^2} + \nu_c \frac{\partial \mathbf{E}(\mathbf{x}, t)}{\partial t} + \omega_p^2 \mathbf{E}(\mathbf{x}, t) \\ = \frac{1}{\mu_0 \epsilon_0} \nabla \times \left( \frac{\partial \mathbf{B}(\mathbf{x}, t)}{\partial t} + \nu_c \mathbf{B}(\mathbf{x}, t) \right) \end{aligned} \quad (9)$$

This expression is used together with Faraday's law used for updating  $\mathbf{B}$  to define the field update equations in the dielectric fluid model. It can be shown that this method exhibits 2nd order accuracy. The demonstration of this accuracy and the details of the approximations used in this model can be found in Schulz et. al. 2004.

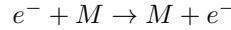
### 3.2. Collisions and air chemistry in the fluid model

Breakdown models for helium, dry air, air with water content, argon and  $\text{SF}_6$  have been developed for the ICEPIC code. These models are valid for atmospheric pressures. The static parameters used in the model are the composition of the gaseous medium, the gas temperature, and the gas density. Several rates have been tabulated in advance so that ICEPIC simulations need only reference look-up tables, instead of numerically solving the Boltzmann

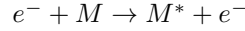
equation on the spot. As a function of the magnitude of the RF field over the pressure  $E/p$ , the look-up tables store the collision frequency, the ionization rate, the electron attachment rates, recombination rates, and the electron temperature. The values in these tables are determined by using the EEDF software package to calculate the electron energy distribution function in the gas mixtures. This is done by using experimentally determined interaction cross sections to numerically solve the steady state Boltzmann equation for the isotropic part of the distribution function.

The dry air model consists of a mixture of  $N_2$ ,  $O_2$ , and  $Ar$  in a ratio of 78/21/1. Several different air chemistry processes are modeled in the fluid breakdown treatment. They are outlined as follows:

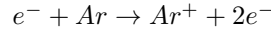
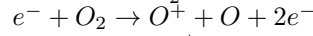
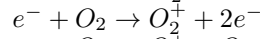
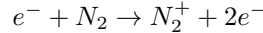
Elastic Collisions



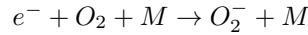
Excitation



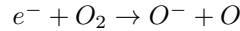
Ionization



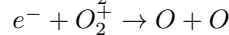
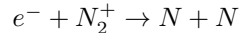
3-Body Attachment



Dissociative Attachment



Recombination



In the ICEPIC simulation, the electron density, collision frequency, and electron temperature are all stored for each cell. The lookup tables are used for all the gas mixtures to evolve the number density of electrons in each timestep according to Eq. (1). From this number density new effective values of  $\omega_p$  and  $\nu_c$  are computed. These quantities are used to update the dielectric constant from Eq. (1). Finally the  $\mathbf{E}$  and  $\mathbf{B}$  fields are advanced in ICEPIC, and the process begins anew.

The air model that includes humidity is tabulated for four possible values of water molecule content; 1%, 2%, 3%, and 4%, where 4% is fully saturated air at room temperature. Since the data are reasonably smooth functions, it is reasonable to interpolate for intermediate values of  $E/p$  and water con-

tent. Water vapor is electronegative, so the effect of introducing it into the gas mixture is to increase the attachment rates. The ionization rate, however, is unaffected by the presence of water vapor. As a result, the breakdown voltage increases with humidity. One effect that has not been implemented yet in this model, however, is the potential presence of water droplets in a humid environment. Because water droplets can create local field enhancements, they can in principle increase the ionization rate. Whether the increase in  $N_e$  due to water droplets is balanced by the decrease due to higher levels of humidity is a matter of some debate, and will be further investigated in future work.

### 3.3. The Particle In Cell (PIC) treatment

ICEPIC computes the time advance of the magnetic field according to Faraday's law, and the electric field according to Ampere-Maxwell's law. The discreet form of these equations used in ICEPIC preserve the constraint equations  $\nabla \cdot \mathbf{B} = 0$  and  $\nabla \cdot \mathbf{E} = \rho/\epsilon_0$  as long as the initial data satisfies these constraints. The particles used in ICEPIC are "macro-particles" that represent many charged particles (electrons and/or ions) with a position vector  $\mathbf{x}$  and a velocity vector  $\mathbf{v} = d\mathbf{x}/dt$ . The relativistic form of Lorentz's force equation is used to determine the particle's velocity:

$$\mathbf{F} = m \frac{d\gamma \mathbf{v}}{dt} = q \left( \mathbf{E} + \frac{\mathbf{v}}{c} \times \mathbf{B} \right) \quad (10)$$

where  $\gamma$  is the usual relativistic factor of  $(1 - v^2/c^2)^{-1/2}$ , and  $q$  and  $m$  are the charge and mass of the particle.

ICEPIC uses a fixed, Cartesian, logical grid to difference the electric and magnetic field equations. The vector quantities  $\mathbf{E}$ ,  $\mathbf{B}$ , and  $\mathbf{J}$  are staggered in their grid location using the technique of Yee 1966.  $\mathbf{E}$  and  $\mathbf{J}$  are located on the edges of the primary grid, whereas  $\mathbf{B}$  is located on the faces of the primary grid. An explicit leap-frog time step technique is used to advance the electric and magnetic fields forward in time. The advantages of the leap-frog method are simplicity and second-order accuracy. The electric field advances on whole integer time steps whereas the magnetic field and the current density advance on half integer time steps.

The three components of the momentum and position of each particle are updated via Eq. (10) using the Boris relativistic particle push algorithm Boris 1970. The particle equations for velocity and position are also advanced with a leap-frog technique. The velocity components are advanced on half integer time steps, and the particle positions are updated on integer time steps. The current density

weighting employs an exact charge conserving current weighting algorithm by Villasenor & Buneman 1992, enforcing  $\nabla \cdot \mathbf{E} = \rho/\epsilon_0$ . Once the particles' positions and velocities are updated and the new current density is updated on the grid, the solution process starts over again by solving the field equations.

### 3.4. Collisions and air chemistry with PIC

The interactions suffered by PIC particles that are being used to model air chemistry are electron-neutral scattering, excitation, and ionization, and ion-neutral scattering, ionization, and charge exchange. Energetic particles that interact with a background gas of neutral atoms have a probability of collision  $P_i$  during a time interval  $\Delta t$  that depends on the number density of background neutral gas molecules  $n_g$ , the energy-dependent cross-section  $\sigma(E_i)$ , and velocity  $v_i$  through the collision frequency of the  $i^{th}$  particle  $\nu_i = n_g(x)\sigma(E_i)v_i$ .

$$P_i = 1 - e^{-\nu_i \Delta t} \quad (11)$$

One scheme for determining whether the  $i^{th}$  particle collides and interacts in a given timestep is to calculate  $P_i$  and compare it with a uniform random number  $R$ . For  $P_i > R$ , the particle will be collided in this time step. However, determining collisions in this way can be computationally expensive. It is substantially less computationally expensive to use the null-collision method in which we compute an energy independent collision frequency:

$$\nu_{null} = \text{MAX}_x(n_g(x))\text{MAX}_E(\sigma(E)v) \quad (12)$$

In this approximation we need not calculate the cross section for every particle in every timestep. Rather, we construct a total collision probability  $P_T$  that represents the fraction of the particles that undergo a collision in a single timestep:

$$P_T = 1 - e^{-\nu_{null} \Delta t} \quad (13)$$

For multiple reactions with the same background gas, the cross-section used in Eq. (12) is a sum of all the individual cross-sections. This method is applied for each background gas in the simulation.

The subset of the total number of particles undergoing a collision in a time step is chosen randomly from the whole set. From this fraction, the energy-dependent cross-section is used to determine if a real collision occurs. Hence, if

$$\frac{n_g(x)\sigma(E_i)\nu_i}{\nu_{null}} > R \quad (14)$$

then a collision occurs. For multiple reactions with the same background gas, the particle must be

tested to see if it under went a reaction with each cross-section that was used to find the cross-section in Eq. (12). Even if the particle undergoes a reaction, it still may experience a different reaction in the same timestep, because it represents many particles.

The ion-neutral collisions are implemented using the same method. For high-energy ions (100kV-500kV), the ion collision frequency is higher than the electron collision frequency.

We have also developed a model based on previous work by Vaughan, Shih, and Gopinath for the secondary electron emission yield  $\delta$ . This model is not used in the breakdown studies presented in this paper, but we mention it because it is a critical part of modeling any experiment that has a vacuum window, such as the bell jar experiments currently being conducted that the Air Force Research Laboratory. The secondary electron emission yield depends on the energy and angle-of-incidence of the primary electron,

$$\delta(E, \Theta) = \delta_{max0} \left( 1 + k_s \frac{\Theta^2}{2\pi} \right) \times f(w, k) \quad (15)$$

where

$$f(w, k) = \begin{cases} (we^{(1-w)})^k & k = \begin{cases} 0.62 & w \leq 1 \\ 0.25 & 1 < w \leq 3 \\ 3.0w^{-0.35} & w > 3 \end{cases} \end{cases} \quad (16)$$

where the energy dependence appears implicitly via

$$w = \frac{E - E_0}{E_{max0} \left( 1 + k_s \frac{\Theta^2}{2\pi} \right) - E_0} \quad (17)$$

#### 4. PRELIMINARY RESULTS

To date we have used both the particle and the fluid breakdown representations to probe transmission through a plasma layer. We have used both implementations to test our hypotheses regarding the functional dependence of the transmission coefficient on the value of the collision frequency. We have also used the fluid representation to simulate the breakdown of a gaseous medium in a two dimensional box. We have observed the growth of the number density of electrons in time and space, and have run the simulation until a steady state is achieved. We have not been able to repeat this portion of the investigation with the PIC representation, because of complications regarding resolution of the Debye length, which we shall summarize along with proposed solutions to the problem.

##### 4.1. The impact of collisions on transmission

To test our hypotheses regarding the dependence of transmission on the collision frequency, summarized in Fig. (2), we have fixed the electron density in the breakdown models. Our results are shown in Fig. (3). It is worth mentioning that  $\omega_p$  in general depends on  $\nu_c$  because  $\nu_c$  enters into the evolution of the number density of electrons. However, since we have fixed  $\omega_p$  in this study, Fig. (3) reflects only the impact of  $\nu_c$  on the mobility and mean free time of the plasma electrons, but not it's changes to  $\omega_p$ . It gives us intuition for how changing the mobility of the electrons affects their efficiency at transferring the RF energy to the background gas (lower values of  $\nu_c$ ), and also how limited mobility impedes their ability to reflect RF energy (higher values of  $\nu_c$ ), but it tells us nothing about how  $\nu_c$ 's changing  $\omega_p$  impacts the fraction of RF energy reflected.

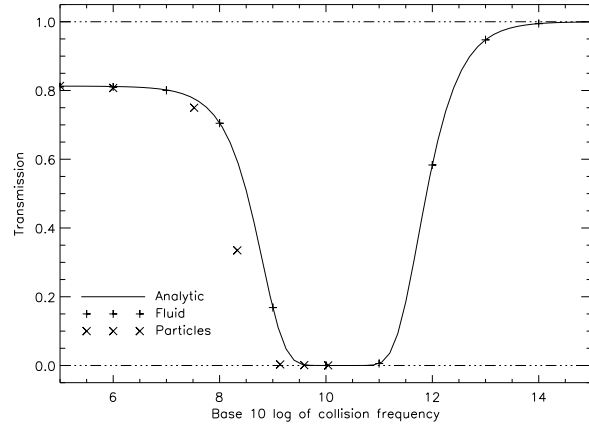


FIG. 3.— The transmission coefficient of an RF signal with  $\omega = 24.98$  GHz as a function of the collision frequency with background neutrals for a fixed plasma density corresponding to  $\omega_p = 21.45$  GHz. Particle collision frequencies have been corrected for grid heating effects.

In the case of the dielectric fluid model, fixing the density is an easy modification, we simply ran the simulations without evolving the number density and keeping the plasma frequency fixed at a particular value, but varying the collision frequency in the dielectric constant from Eq. (1). In the PIC case we have artificially enforced that the number density remain the same by allowing momentum scattering collisions to take place, but not adding another particle to the simulation. Changes to the collision frequency were accomplished by making the corresponding change to the interaction cross section. The results from the PIC computation require a more sophisticated interpretation, however, because in these runs we had insufficient computational resources to adequately resolve the Debye length. The effect of this lack of resolution of the

Debye shielding is that particles in the simulation experience electromagnetic forces from other particles that ought to have been shielded, which causes all the particles in the simulation to heat. The collision frequency in the PIC representations depends on the temperature as well as on the cross section  $\sigma$ , according to the formula

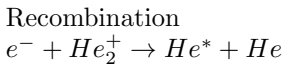
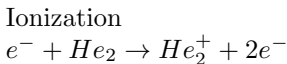
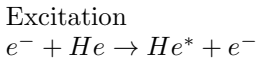
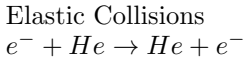
$$\nu_c = \frac{m_e \sigma^2}{3k_B T_e n_g} \quad (18)$$

Therefore, a correction for the particle heating was introduced in order to properly plot transmission versus collision frequency. The correction we applied was a very rough one, essentially taking the average temperature of all the particles in the simulation at the very end of the run, and using that temperature along with the cross section we supplied to calculate  $\nu_c$ , the independent variable in Fig.(4).

Another difficulty with the particle simulations occurs when the collision frequency grows enough to require multiple collisions per cell, per timestep of the simulation. This essentially causes the run time to increase dramatically, and we did not complete any simulations for collisions frequencies past this threshold. In future it would be extremely useful to probe this part of the parameter space with the particle collision model, therefore the development of a more efficient treatment of particle collisions is a matter of current investigation.

#### 4.2. Breakdown simulation in a 2 dimensional box

In a second study we conducted a full breakdown simulation of an RF signal incident upon a region of helium gas in a 2-D box. We chose to study helium because there are fewer interaction processes and thus it was one of the first to be tabulated and implemented in ICEPIC. The interactions modeled in the helium breakdown are



The geometry used in the simulation is shown in Figure (4). The probe recording the transmitted signal is placed in the right vacuum outside the

helium layer, but within the plane wave launching boundary. The probe measuring the reflected signal is in the left vacuum outside the plane wave launcher, to avoid interference with the incident wave.

To study the breakdown, we made movies of the  $|\mathbf{E}|$  field in the box, and observed the process as the RF energy was first attenuated in the helium, and later reflected, and finally reached a steady state with some fraction being transmitted through, and a larger fraction being reflected back toward the source. We also made a simultaneous movie of the density of free electrons in the plasma, which was very helpful in understanding the various stages in the  $|\mathbf{E}|$  field movie.

In the beginning of the simulation, the RF wave hits the helium layer and initially passes directly through it virtually unaffected. In the electron density movie however, the electron density begins to grow at a constant rate throughout the medium. The electron density is higher at the left edge of the helium layer than further in because more of the wave causing the ionization has passed by that point. After some time, the amplitude of the RF signal begins to get attenuated, and simultaneously in the density movie, the density of electrons near the vacuum-helium interface begins to grow exponentially. This attenuates the wave enough that the density further into the helium layer stops growing and in some cases, may even decrease. This happens because the signal that was driving the ionization of the background gas is no longer strong enough to do so. From this time forward, any fraction of the RF signal that makes it through the high density region at the left interface with the vacuum propagates without any significant attenuation through the rest of the helium layer. The action at the interface has just begun, however. As the electron density grows exponentially, the surface of the plasma

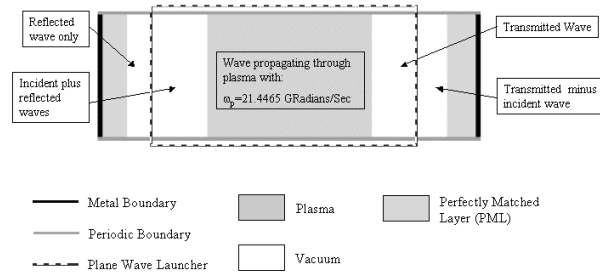


FIG. 4.— A helium layer lies between two vacuum regions. The dashed line represents the plane wave launching boundary, which emits on the left and absorbs on the right. The top and bottom boundaries of the simulation are periodic, while the left and right boundaries are metallic but shielded with a Perfectly Matched Layer (PML) that attenuates all EM signals to 30 db.

becomes much more efficient at reflecting the signal, and thus the  $\mathbf{E}$  field movies shows a growth in the reflected power and a corresponding decrease in the net transmitted signal. This causes the exponential growth of the electron density near the boundary to cease, and eventually a stable equilibrium is reached with a static distribution in the electron density, and a fixed ratio between the transmitted and reflected signals. Figs. (5) and (6) are frames from the  $\mathbf{E}$  field and electron density movies, and show the long term steady state equilibrium that is reached in the field values and density distribution.

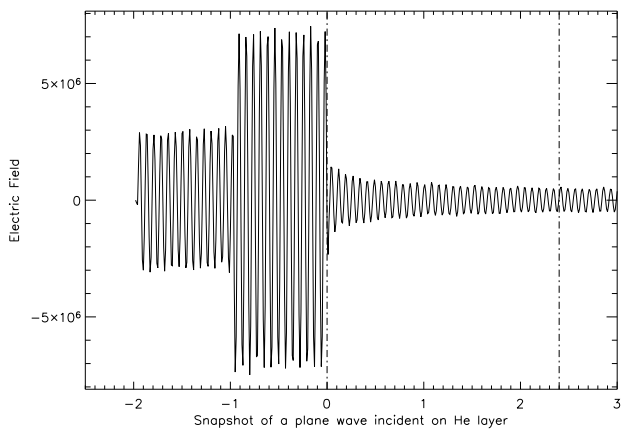


FIG. 5.— This is a snapshot of the traveling E-M wave through the helium layer. The helium is located between 0 and 2.4 on the plot. The wave emitter is located at the position -1. The signal between -2 and -1 is traveling from right to left, and represents the net reflected signal from the helium layer. The wave between -1 and 0 is the interference between the incident and reflected waves, currently undergoing constructive interference. The transmitted signal is measured outside the helium, in the region between 2.4 and 3.

It would have been a nice experiment to repeat this analysis using the PIC representation of breakdown physics, and compare the predictions of each model quantitatively. This has turned out to be a serious challenge for the following reasons. First, by examining the density plot in Fig (6) it is clear that the number of particles has grown over several orders of magnitude since the simulation began. This presents a problem for PIC not only because there are so many particles, but because these high densities require very fine resolution in the mesh to adequately resolve the Debye length. Simulations run without resolution of the Debye Length at the densest regions are subject to severe grid heating of the particles, which in turn affects the collision frequency with the background gas, and in general causes incorrect predictions in the physics. Even though the physical area that requires this high level of resolution is only a small fraction of the total simulation area, ICEPIC does not yet have adaptive

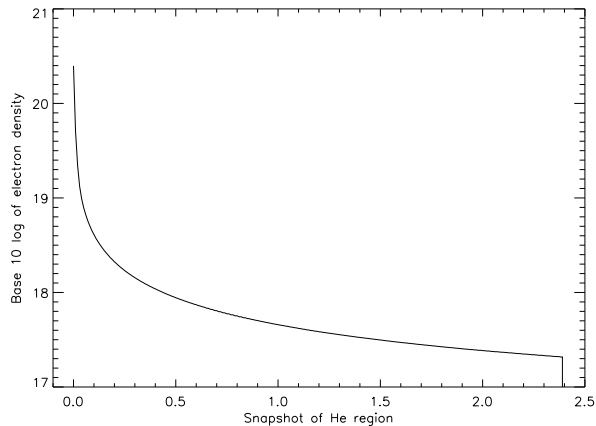


FIG. 6.— This is a snapshot of the density profile of the free electrons in the plasma. This illustrates why most of the RF signal is reflected or attenuated between 0 and 0.2. The initial density profile was flat at  $0.5 \times 10^{16}$  throughout the helium. The RF signal drove a constant growth in density until the exponential growth at the left interface prevented sufficient transmission to continue ionizing the plasma further in.

mesh capability, and would thus require that we resolve the entire domain on this small scale. Another difficulty is that the collision frequency is growing substantially throughout the simulation. When the collision frequency becomes so high that random numbers must be generated many times for each cell in each timestep, it causes the simulation to grind to a near halt. However, there is yet hope. The breakdown simulation performed with the bulk model suggests that the majority of the interesting physical phenomena take place within a short distance of the interface with the vacuum. Thus, it is not necessary to simulate such a vastly large gaseous layer, and we may be able to compare direct results between the PIC and fluid breakdown models if we model transmission through a very thin region. To do this successfully however will still require that we develop a better way to model multiple collisions per timestep in the PIC regime. These subjects are currently under investigation by our group.

Another approach we are currently investigating is to try to employ both the PIC and the fluid modeling of breakdown simultaneously in a hybrid treatment. This is advantageous because while the fluid modeling alone is valid for some electron energy distributions such as Maxwellian or Druyvesteyn, it does not model the case when a secondary population of very high energy electrons develops in the breakdown. We suspect that much of the interesting physics driving the breakdown is governed by these high energy electrons, and are working on using PIC particles to model them while using the fluid to model the remaining population in the



plasma. Some preliminary work on this approach can be found in Schulz et. al. 2004.

## 5. CONCLUSIONS AND FUTURE WORK

We have presented here some background in breakdown theory, and two methods for numerically modeling RF breakdown. We have predicted that RF breakdown depends in a significant way on the collision frequency of electrons in the plasma with the background gas molecules, and have demonstrated that both PIC and fluid breakdown models reproduce this dependence. Of particular interest is the result that a high collision frequency can mitigate the attenuation of the transmitted signal. Even in the case where the plasma frequency exceeds the RF frequency, transmission through the plasma layer can be achieved if the density of the background gas is large enough to restrict the mobility of the plasma electrons. We suggest that in this range of parameters, “breakdown” does not occur because the RF signal is able to propagate through the medium.

We have also reported on the results of a preliminary breakdown computation in a helium background gas. We have discovered several stages in the breakdown process; the homogeneous heating and ionization of the background gas, the exponential breakdown of a thin layer just at the surface of the vacuum-helium interface, the resulting lack of transmitted power into the interior of the gas causing a relaxation of the ionization rate everywhere but at the interface, the reflection of an increasing fraction of the RF power by the surface plasma layer, and the eventual stabilization into an equilibrium with fixed density profile and ratio of reflected to transmitted power. We were interested to find that once equilibrium is reached, almost all of the signal attenuation occurs at the vacuum-helium interface because the density is several orders of magnitude larger there than anywhere else in the gas.

We experienced much difficulty in reproducing the breakdown simulation with the PIC model we have developed. This is because the exponential growth in density at the interface with the vacuum causes the simulation to slow down a considerable amount. The density growth also causes the Debye length to shrink, and at later stages in the simulation we are no longer resolving it, resulting in spurious heating of the simulation particles. Finally, for very large values of the collision frequency, the random number generation for collisions in each cell begins to dominate the total run time, causing this method to become impractical.

In future, we will find a valid statistical approach

to simulating PIC collisions in the range of parameters requiring multiple collisions per cell per timestep. Having learned that most of the interesting breakdown physics occurs in a very thin layer of gas, we will modify our simulation geometry in an attempt to draw a direct comparison between our two methods. We will continue our PIC-fluid hybridization efforts in an attempt to simultaneously capture all the relevant physics. We will study breakdown in air rather than helium, and investigate the effects of introducing humidity, water droplets, and dust. We would also like to investigate pulsed RF signals, and contrast their impact on breakdown to the continuous wave results. In the long term, once we have bench-marked this machinery and compared it to the results of air breakdown experiments currently being designed at the Air Force Research Laboratory, we can incorporate this technology into the virtual prototyping of future high power microwave weapons.

The authors would like to thank Dr. Peter J. Turchi for useful discussions on this work. This research was supported in part by Air Force Office of Scientific Research (AFOSR).

## REFERENCES

- Anderson, D., Lisak, M., Lewin, T., “Breakdown in Air Filled Microwave Waveguides During Pulsed Operation,” *App. Phys.* 56, (1984)
- Boris, J.P., “Relativistic Plasma Simulation-Optimization of a Hybrid Code,” *Num. Sim. Plasmas*, Navan Res. Lab., Wash D.C., (1970) 3-67
- Schulz A.E., Greenwood, A.D., Cartwright, K.L., Mardahl, P.J., “Hybrid Particle-Fluid Modeling of Plasmas,” preprint xxx.lanl.gov/physics/0402045
- Villasenor, J., Buneman, O., “Rigorous Charge Conservation for Local Electromagnetic Field Solvers,” *Comp. Phys. Comm.*, **69** (1992) 306
- Yee, K.S., “Numerical Solution of Initial Boundary Value Problems Involving Maxwell’s Equations in Isotropic Media,” *IEEE Trans. Ant. Prop.*, **AP-14** (1966) 302